SUGISAKA MASANORI

Journal of Robotics, Networking and Artificial Life Vol. 10(4); March (2024), pp. 374–382
ISSN (Online): 2352-6386; ISSN (Print): 2405-9021
https://alife-robotics.org/jrnal.html

Research Article

Modeling of Contactless Ground Speed Sensor

Jakaria Mahdi Imam[1], Mohammad Aminul Islam[1], Norrima Mokhtar[1], S. F. W. Muhammad Hatta[1], Heshalini Rajagopal[2]
[1]*Department of Electrical Engineering, Faculty of Engineering, 50603 University of Malaya, Malaysia*
[2]*Department of Electrical & Electronic Engineering, Mila University, Negeri Sembilan, Malaysia*

ARTICLE INFO

Article History

Received 24 November 2023
Accepted 25 July 2024

Keywords

Contactless speed sensor
Vessels
Submarine
Aircraft
Navigation

ABSTRACT

The proposed novel contactless speed sensor sounds intriguing and presents potential advantages over the conventional methods used in vessels, submarines, and aircraft. It is asserted that the utilization of a small-sized ball, dropped within a vacuum chamber, enables the direct measurement of the ground speed of these vehicles, as opposed to their speed relative to the water or air. This could be a significant improvement, as ground speed is often more relevant for navigation and operational purposes. A useful method for assessing the practicality and accuracy of the suggested sensor is to use simulation to verify its conceptual and mathematical model. However, it's important to note that simulations are different from real-world testing, and further experimental verification would be necessary to confirm the reliability of the sensor under various conditions and environments. One major advantage of this proposed sensor is its independence from the operational environment. Unlike current speed sensors that require contact with the air or water, the suggested sensor can be placed entirely inside the vehicle. By eliminating the necessity to mount the sensor externally, the risk of collision with external objects is minimized, resulting in an enhanced overall safety of the system.

1. Introduction

Currently, submarines and vessels rely on various speed sensors like Electromagnetic Log (EM Log) and Pitometer Log for speed measurement [1], [2], [3]. However, these devices are capable to quantify the vessel's speed relative to the water only and not the ground. Consequently, due to factors like tides or currents, vessels cannot directly quantify their speed with respect to the ground [4]. For example, a ship's speed sensor may report a high speed even when the ship is motionless relative to the ground when it anchors at sea while under the influence of a strong current [5]. Similarly, an aircraft's pilot tube is used to gauge its speed in relation to the air, not the ground [6], [7]. It follows that because of the effect of air, aircraft are unable to determine their speed in relation to the ground directly [8], [9], [10], [11]. Fig.1 shows the current technique that ships use to gauge their land speed. Currently, the EM Log speed, propeller speed, wind sensor, and tide table data are taken into account when determining a vessel's ground speed [5]. Nevertheless, due to inaccuracies in the EM Log and Tide Table, this method results in considerable errors in

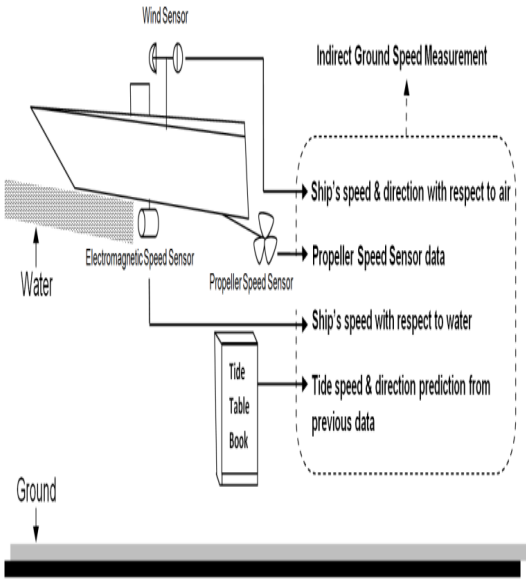

Fig.1 Prevailing approach utilized by vessels to measure ground speed

Corresponding author E-mail: norrimamokhtar@um.edu.my

ground speed measurement [1].

We highlighted some important challenges faced by vessels, submarines, and aircraft in measuring their ground speed, particularly when GPS and external sources are unavailable. As inaccurate input parameters can result in large mistakes when estimating ground speed, relying on air speed, altitude, pressure, density, and other onboard sensor information is a risk. These errors can potentially impact navigation and operational decisions, making direct ground speed measurement highly desirable. The accuracy problems associated with air and water vehicles might be further aggravated by the fact that existing speed sensors are environment dependent. These sensors require contact with the operational environment, which means they are influenced by factors such as temperature, density, salinity, and chemical properties. These environmental variations can introduce uncertainties in the speed measurements, affecting the overall reliability of the sensor. Additionally, the placement of these external sensors or their probes outside the vehicle poses potential risks of collision with external objects, especially in situations where vehicles operate in confined or busy spaces.

Considering these challenges, a contactless speed sensor that directly measures ground speed without relying on environmental parameters and without the need for external probes would be a significant advancement. The proposed novel sensor, mentioned in the previous discussion, has the potential to address these issues by offering a different approach to ground speed measurement.

However, as with any new technology, it is essential to thoroughly validate the proposed sensor's theoretical model and simulate its performance in various scenarios. Experimental verification and real-world testing will be crucial to confirm its accuracy, reliability, and practicality before considering its widespread adoption in critical applications like aviation, naval operations, and maritime navigation.

Overall, finding a solution to directly measure ground speed without environmental dependencies and external probes would be highly valuable, contributing to safer and more efficient operations of vessels, submarines, and aircraft in situations where GPS and external sources are not available or are unreliable.

GPS serves as a means for measuring ground speed, however this is not suitable for vessels and aircraft as it is vulnerable to blocking and spoofing [12], [13]. Moreover, when submarines operate underwater, GPS functionality becomes ineffective [14]. In some rare cases, vehicles may employ accelerometers for ground speed measurement [15], [16]. However, relying solely on accelerometers leads to increased inaccuracies over time due to various biases, noise, and errors associated with these sensors [17]. Consequently, accelerometers are often used in conjunction with other devices to quantify ground speed [15], [16], [17]. The speed of water and air vehicles with respect to the ground cannot be directly measured by any environment-independent, contactless, individual onboard speed sensor that we are aware of. Our proposal aims to bridge this gap by creating a new approach for a standalone onboard speed sensor that is contactless and environment independent. It functions similarly to a standalone accelerometer or gyro sensor. Without the need for additional data, such propeller RPM or current speed, this sensor can estimate the speed of water and air vehicles in relation to the ground directly.
In this paper, a novel invention—a contactless speed sensor that can monitor an aircraft's, submarine's, or vessel's ground speed directly—is presented. By eliminating the environmental dependency, it can potentially offer more accurate and reliable speed measurements, which are crucial for navigation and operational purposes. The emphasis on a theoretical and mathematical model is essential for understanding the underlying principles and ensuring the device's accuracy and effectiveness. Validating this model through simulation is a necessary step to assess the sensor's performance under various conditions and scenarios. However, as previously mentioned, simulations are not a substitute for real-world testing. Therefore, it would be valuable to complement the simulation results with experimental data to confirm the practical applicability and accuracy of the sensor.

2. Methodology

2.1. *Theoretical Foundation*

The principle of compound motion, which was developed by Galileo in 1638 [18] stated that the vertical motion (velocity in the z-axis) and the horizontal motion (velocity in the x and y axes) are totally independent of one another in projectile motion. To further understanding, let us think about an item in free fall on Earth that is in a vacuum. Table 1 [18] presents the object's 3-axis, x, y, and z axis velocity characteristics based on Galileo's discoveries.

Table 1 Properties of the item in an airless atmosphere while it is falling freely.

Time (Sec)	Velocity in x-Axis (m/s)	Velocity in y-Axis (m/s)	Velocity in z-Axis (m/s)
0.1	5	10	0.98
0.2	5	10	1.96
0.3	5	10	2.94
0.4	5	10	3.92
0.5	5	10	4.9
0.6	5	10	5.88
0.7	5	10	6.86
0.8	5	10	7.84
0.9	5	10	8.82
1.0	5	10	9.8

Table 1 shows that when an item is in free fall without any external resistance, gravity has no effect on its horizontal velocity (velocity along the x and y axes), which means that the object's velocity remains constant throughout time. But the force of gravity may alter the vertical velocity, or the velocity along the z-axis. This suggests that the item's x and y-axis velocities will not change after we quantify them until the thing touches the earth. By placing tiny free-falling balls inside a vacuum chamber, this idea raises the possibility of developing a unique sensor. This sensor would make it possible to monitor a vehicle's horizontal velocity in relation to the ground (along the x and y axes) directly.

2.2. Proposed Speed Sensor

In light of the previous discussion, the speed sensors that are now in use for air and water vehicles are unable to assess ground speed directly, requiring interaction with the surrounding environment. To estimate ground speed indirectly, they rely on extra data, such as propeller speed data, tide table data, etc. (Fig. 1). On the other hand, no other information such as propeller speed or tide table data is required for the proposed speed sensor to measure ground speed directly. Moreover, it does not necessitate direct physical contact with the operational environment, which makes it extremely adaptable and simple to install at any suitable place aboard the vessel (Fig. 2).

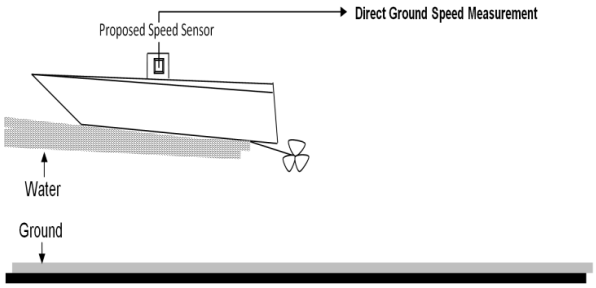

Fig. 2 The proposed contactless speed sensor is positioned within the vessel to directly measure ground speed

A schematic of the recommended speed sensor's basic configuration is shown in Fig. 3. The mechanism consists of a continuous free-fall ball descending inside an enclosed vacuum chamber. Within the vacuum chamber, the balls descend in a single line from the top and are redirected back to the top once they reach the bottom. The arrangement ensures that a minimum of 2 balls are consistently in a state of free fall. Positioned along the boundary of the vacuum chamber is a 3D Range Finder, which can accurately measure the 3D distance of at least 2 free-falling balls simultaneously.

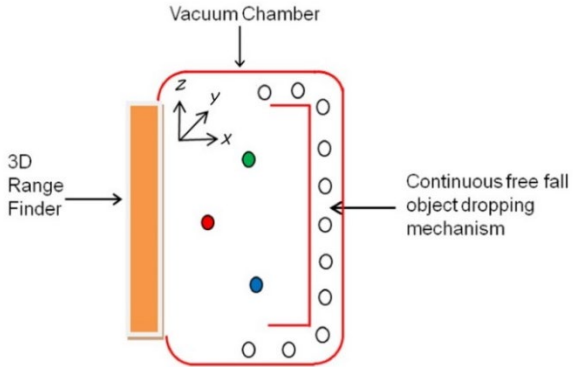

Fig.3. Fundamental setup of the sensor

2.3. *Operating Principle*

To facilitate comprehension, we will begin by examining a single free-falling ball as depicted in Fig. 4. Following that, we will delve into the discussion of multiple free-falling balls using Fig. 5.

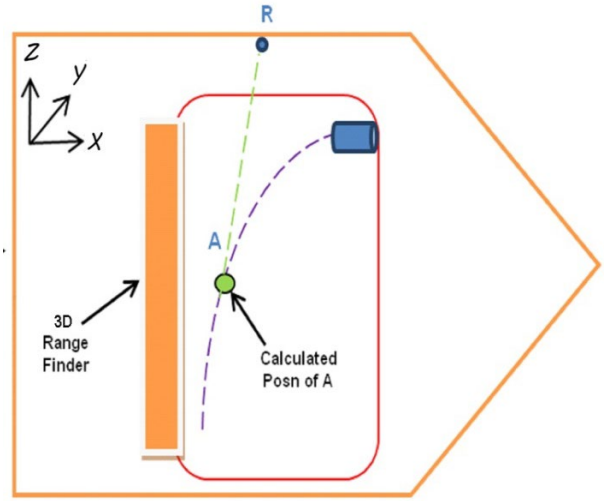

Fig. 4 Setup of sensor in the vehicle.

The sensor unit is first put inside the car and carefully aligned in all three directions. Three key pieces of data are required for the system to function: the gravity model, the vehicle's 3-axis orientation with respect to Earth, and the ongoing measurement of the relative distance between the vehicle and the falling ball. A 3-axis gyro may be utilised to determine the vehicle's 3-axis global orientation. A 3-axis accelerometer may be used to determine the Gravity model. Using a proper 3D range finder, one may measure the relative distance between the vehicle (point R) and the falling ball. Ball A, the initial ball, starts to descend as soon as the sensor is working. Ball A keeps the same velocities along the x and y axes as it descends freely, as indicated in Table 1, with respect to the earth, until it reaches the vacuum chamber. Only once, at the start of the process (time t0), must Ball A's x and y-axis velocities relative to the ground be obtained

from outside sources (like GPS). After that, the velocities won't require any more input, therefore these other sources won't be necessary.

We can predict Ball A's future horizontal velocities with respect to the ground using simple mathematical equations and the data in Table 1 once we have the horizontal velocities of the ball along both axes at a particular time (t0). This allows us to avoid relying on any external sensors. Therefore, Ball A can act as a reliable reference for ground speed.

Let us examine an example where the vehicle starts to go in different directions and at varied speeds immediately after time zero in order to improve understanding. We can use Ball A as a speed reference if we can determine the relative distance between Ball A and the car at two different points in time. This allows us to calculate the average horizontal velocity of the vehicle along the two axes between those two moments. Once Ball A makes contact with the vacuum chamber at the conclusion of its free fall, it loses its ability to serve as a speed reference. A continuous loop made up of several falling balls (like Ball A) grouped in a single line is added to keep a continuous measurement of the vehicle's velocity, as shown in Fig. 5.

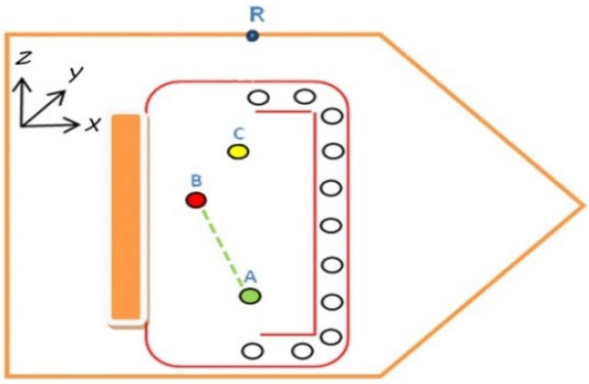

Fig. 5 Multiple free-falling balls operating inside the sensor

The loop is designed to maintain a minimum of two balls in free fall at all times. Ball B will be the next ball to start falling free after Ball A, and Ball B will become the new point of reference for calculating the vehicle's 2-axis horizontal velocity. Ball A cannot reach the bottom until this change in reference takes place. Ball B's 2-axis horizontal velocity becomes the new benchmark for all subsequent measurements once it is determined. We apply the same technique that was utilised to obtain the vehicle's 2-axis horizontal velocity to ascertain Ball B's 2-axis horizontal velocity. Using the same 3D range finder, we can determine the 2-axis horizontal velocity of Ball B with respect to falling Ball A by measuring the 2-axis (horizontal) relative distance between falling Ball B and falling Ball A at two separate time periods.

Ball B becomes the new reference after its 2-axis horizontal velocity is obtained, replacing ball A. For the purpose of calculating the vehicle's 2-axis average horizontal velocity, ball B now fulfils the same function as ball A. Subsequent balls—C, D, E, F, G, H, and so on—continue the procedure. The suggested speed sensor's flowchart is shown in Fig.6.

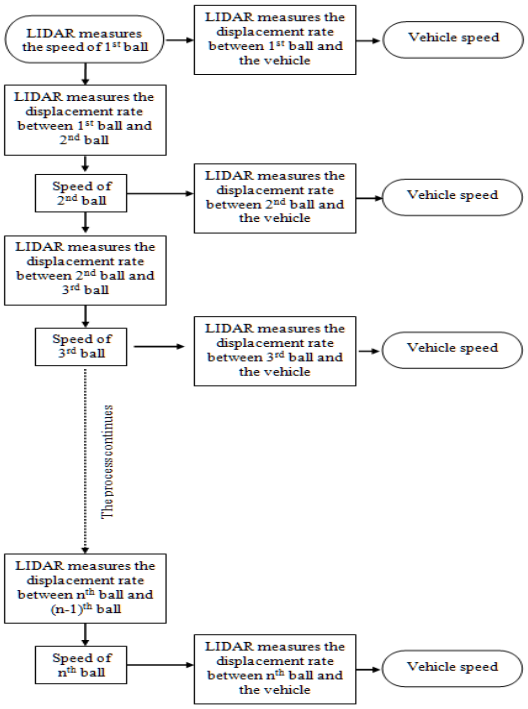

Fig.6.Flowdiagram of the proposed speed sensor

2.4. *Mathematical Modeling*

Table 2 depicts the notations of the parameters used in this work. We know from the beginning that ball A is descending with a 2-axis horizontal velocity. Assume that at time t_0, we observed its velocities along the x and y axes, which we recorded as $v_{A_{xt0}}$ and $v_{A_{yt0}}$, respectively. Using Eqs. 1 and 2, we can predict ball A's horizontal velocities along the x and y-axis at any later time t_1, provided it stays in free fall and doesn't touch the bottom.

$$v_{A_{xt1}} = v_{A_{xt0}} \quad (1)$$

$$v_{A_{yt1}} = v_{A_{yt0}} \quad (2)$$

Similarly, using Eqs. 3 and 4, we may forecast the 2-axis horizontal velocity of falling ball A at time t2:

$$v_{A_{xt2}} = v_{A_{xt1}} = v_{A_{xt0}} \quad (3)$$

$$v_{A_{yt2}} = v_{A_{yt1}} = v_{A_{yt0}} \quad (4)$$

Table 2. Notations used in this work

Symbol	Meaning
T	Time (second)
v_{M_x}	Velocity of the current ref ball on x-axis (m/s)
v_{M_y}	Velocity of the current ref ball on y-axis (m/s)
d_{RM_x}	Distance between current ref ball and vehicle ref point R on x-axis (m)
d_{RM_y}	Distance between current ref ball and vehicle ref point R on y-axis (m)
v_{V_x}	Velocity of the vehicle on x-axis (m/s)
v_{V_y}	Velocity of the vehicle on y-axis (m/s)
d_{NM_x}	Distance between current ref ball and next ball on x-axis (m)
d_{NM_y}	Distance between current ref ball and next ball on y-axis (m)
v_{N_x}	Velocity of the next ref ball on x-axis (m/s)
v_{N_y}	Velocity of the next ref ball on y-axis (m/s)

Our goal at this stage is to measure, at two different times, t1 and t2, the relative distance along the horizontal two axes between the falling ball A and the vehicle's reference point R. Assuming that the horizontal 2-axis relative distance of the falling ball A from the vehicle's reference point R at times t_1 and t_2 was correctly measured, the results are represented as, t_1 and t_2 as $d_{RA_{xt1}}$, $d_{RA_{yt1}}$ and $d_{RA_{xt2}}$, $d_{RA_{yt2}}$, respectively. Eqs. 5 and 6 may be used to determine the vehicle's 2-axis average horizontal velocity between times t_1 and t_2 based on the available data.

$$v_{V_{x(t1\,\&\,t2)}} = v_{A_{xt2}} - \{d_{RA_{xt2}} - d_{RA_{xt1}}) / (t_2 - t_1) \quad (5)$$

$$v_{V_{y(t1\,\&\,t2)}} = v_{A_{yt2}} - \{d_{RA_{yt2}} - d_{RA_{yt1}}) / (t_2 - t_1)\} \quad (6)$$

Likewise, we may continue to ascertain the vehicle's 2-axis average horizontal velocity between periods t_2 and t_3, t_3 and t_4, t_4 and t_5, and so on until t_{n-1} and t_n. Eqs. 7, 8, 9 and 10 can be used to simplify them.

$$v_{A_{xtn}} = v_{A_{xt(n-1)}} \quad (7)$$

$$v_{A_{ytn}} = v_{A_{yt(n-1)}} \quad (8)$$

$$v_{V_{x(tn-1\,\&\,tn)}} = v_{A_{xtn}} - \{(d_{RA_{xtn}} - d_{RA_{xtn-1}})/(t_n - t_{n-1})\} \quad (9)$$

$$v_{V_{y(tn-1\,\&\,tn)}} = v_{A_{xtn}} - \{(d_{RA_{ytn}} - d_{RA_{ytn-1}})/(t_n - t_{n-1})\} \quad (10)$$

Assume that ball B will emerge at time t_6. Measured at time t_6, the 2-axis (horizontal) relative distance between falling ball B and falling ball A is $d_{BA_{xt6}}$, $d_{BA_{yt6}}$ and measured at time t_7, is $d_{BA_{xt7}}$, $d_{BA_{yt7}}$. Thus, at time t_7, Eqs. 11 and 12 may be used to get the 2-axis horizontal velocity of the falling ball B.

$$v_{B_{xt7}} = v_{A_{xt6}} + \{(d_{BA_{xt7}} - d_{BA_{xt6}})/(t_7 - t_6)\} \quad (11)$$

$$v_{B_{yt7}} = v_{A_{yt6}} + \{(d_{BA_{yt7}} - d_{BA_{yt6}})/(t_7 - t_6)\} \quad (12)$$

The above equations can be simplified as Eqs. 13 and 14:

$$v_{B_{xtn}} = v_{A_{xtn-1}} + \{(d_{BA_{xtn}} - d_{BA_{xtn-1}})/(t_n - t_{n-1})\} \quad (13)$$

$$v_{B_{ytn}} = v_{A_{ytn-1}} + \{(d_{BA_{ytn}} - d_{BA_{ytn-1}})/(t_n - t_{n-1})\} \quad (14)$$

The following ball becomes the current reference point after its 2-axis horizontal velocity is determined. Thus, in the continuous falling ball system, the 2-axis horizontal velocity of this current reference may be predicted at any given time using Eqs. 15 and 16:

$$v_{N_{xtn}} = v_{M_{xtn-1}} + \{(d_{NM_{xtn}} - d_{NM_{xtn-1}})/(t_n - t_{n-1})\} \quad (15)$$

$$v_{N_{ytn}} = v_{M_{ytn-1}} + \{(d_{NM_{ytn}} - d_{NM_{ytn-1}})/(t_n - t_{n-1})\} \quad (16)$$

Eqs. 17 and 18 may be used to express the vehicle's 2-axis average horizontal velocity in a continuous falling ball system.

$$v_{M_{xtn}} = v_{M_{xtn-1}} \quad (17)$$

$$v_{M_{ytn}} = v_{M_{ytn-1}} \quad (18)$$

Ball B can take the place of ball A as the new speed reference after its 2-axis horizontal velocity has been established. In accordance with this arrangement, the reference will proceed to move successively to balls C to H, and so forth. In a continuous falling ball system, if we designate the present ball as M and the next ball as N, we have to figure out the 2-axis horizontal velocity of the next ball using the current ball as a reference. Eqs. 19 and 20 can be used to express the reference shifting equations in this case:

$$v_{V_{x(tn-1\,\&\,tn)}} = v_{M_{xtn}} - \{(d_{RM_{xtn}} - d_{RM_{xtn-1}})/(t_n - t_{n-1})\} \quad (19)$$

$$v_{V_{y(tn-1\,\&\,tn)}} = v_{M_{ytn}} - \{(d_{RM_{ytn}} - d_{RM_{ytn-1}})/(t_n - t_{n-1})\} \quad (20)$$

3. Results and discussion

A computer simulation was developed using the MIT Scratch program with the goal of verifying the theoretical and mathematical model of the suggested sensor. In order to assess the mathematical equations given in the mathematical modelling section, the simulation included situations involving both stationary and moving vehicles. Meters were used to measure lengths and meters per

second (m/s) to measure velocity. The sensor assembly was put inside a car with zero velocity in each of the three axes for the static test, thus the sensor was not exposed to this velocity data. Table 3 displays the outcomes of the Static Test simulations. The sensor system was mounted inside a vehicle that ran at steady speeds of 5 m/s along the x-axis and 10 m/s along the y-axis during the dynamic test. Interestingly, this velocity data was unavailable to the sensor. Table 4 shows the results of the Dynamic Test simulation. Using Eqs. 19 and 20, respectively (the v_{V_x} and v_{V_y} columns of Table 3, the sensor successfully determined the vehicle's velocities as 0 m/s on the x-axis and 0 m/s on the y-axis during the static test.

Similar to this, the sensor accurately calculated the vehicle's velocities in the dynamic test, using Eqs. 19 and 20, respectively, for the x- and y-axes, v_{V_x} and v_{V_y} columns of Table 4. The sensor was kept in the dark about the vehicle velocities for the several executions of the dynamic test, which had cars travelling at different constant speeds. The sensor correctly calculated the vehicle's velocity in every case. The conceptual results of the simulations showed that the proposed sensor could measure the speed of water and air vehicles in relation to the ground directly. Unlike traditional sensors, this one doesn't need to be installed outside of the car or utilise external probes. Unlike existing speed sensors, the complete sensor unit may be positioned within the

Table 3. Simulation results of the static test

Sample No.	T (s)	v_{M_x} (m/s)	v_{M_y} (m/s)	d_{RM_x} (m)	d_{RM_y} (m)	v_{V_x} (m/s)	v_{V_y} (m/s)	d_{NM_x} (m)	d_{NM_y} (m)	v_{N_x} (m/s)	v_{N_y} (m/s)	Observation
				(15)								
1st Ball is used as a reference												
1	0.1	10	10	1	1	0	0					
2	0.2	10	10	2	2	0	0					
3	0.3	10	10	3	3	0	0					
4	0.4	10	10	4	4	0	0					
5	0.5	10	10	5	5	0	0	4	4			2nd Ball appeared
6	0.6	10	10	6	6	0	0	4	4	10	10	
7	0.7	10	10	7	7	0	0	4	4	10	10	
8	0.8	10	10	8	8	0	0	4	4	10	10	
9	0.9	10	10	9	9	0	0	4	4	10	10	
2nd Ball is used as a reference as 1st Ball is lost												
10	1.0	10	10	6	6	0	0					
11	1.1	10	10	7	7	0	0	6	6			3rd Ball appeared
12	1.2	10	10	8	8	0	0	6	6	10	10	
13	1.3	10	10	9	9	0	0	6	6	10	10	
3rd Ball is used as a reference as 2nd Ball is lost												
14	1.4	10	10	4	4	0	0					
15	1.5	10	10	5	5	0	0	4	4			4th Ball appeared
16	1.6	10	10	6	6	0	0	4	4	10	10	
17	1.7	10	10	7	7	0	0	4	4	10	10	
18	1.8	10	10	8	8	0	0	4	4	10	10	
19	1.9	10	10	9	9	0	0	4	4	10	10	
4th Ball is used as a reference as 3rd Ball is lost												
20	2.0	10	10	6	6	0	0					
21	2.1	10	10	7	7	0	0	6	6			5th Ball appeared
22	2.2	10	10	8	8	0	0	6	6	10	10	
23	2.3	10	10	9	9	0	0	6	6	10	10	
5th Ball is used as a reference as 4th Ball is lost												
24	2.4	10	10	4	4	0	0					
25	2.5	10	10	5	5	0	0	4	4			6th Ball appeared
26	2.6	10	10	6	6	0	0	4	4	10	10	
27	2.7	10	10	7	7	0	0	4	4	10	10	
28	2.8	10	10	8	8	0	0	4	4	10	10	
29	2.9	10	10	9	9	0	0	4	4	10	10	
6th Ball is used as a reference as 5th Ball is lost												
30	3.0	10	10	6	6	0	0					
31	3.1	10	10	7	7	0	0	6	6			7th Ball appeared
32	3.2	10	10	8	8	0	0	6	6	10	10	
33	3.3	10	10	9	9	0	0	6	6	10	10	
7th Ball is used as a reference as the 6th Ball is lost												
.												
.												
.												
nth Ball is used as reference when (n-1)th Ball is lost												

Table 4. Simulation results of the dynamic test

Sample No.	T (s)	v_{M_x} (m/s)	v_{M_y} (m/s)	d_{RM_x} (m) (15)	d_{RM_y} (m)	v_{V_x} (m/s)	v_{V_y} (m/s)	d_{NM_x} (m)	d_{NM_y} (m)	v_{N_x} (m/s)	v_{N_y} (m/s)	*Observation*
1st Ball is used as a reference												
1	0.1	15	20	1	1	5	10					
2	0.2	15	20	2	2	5	10					
3	0.3	15	20	3	3	5	10					
4	0.4	15	20	4	4	5	10					
5	0.5	15	20	5	5	5	10	4	4			2nd Ball appeared
6	0.6	15	20	6	6	5	10	4	4	15	20	
7	0.7	15	20	7	7	5	10	4	4	15	20	
8	0.8	15	20	8	8	5	10	4	4	15	20	
9	0.9	15	20	9	9	5	10	4	4	15	20	
2nd Ball is used as a reference as 1st Ball is lost												
10	1.0	15	20	6	6	5	10					
11	1.1	15	20	7	7	5	10	6	6			3rd Ball appeared
12	1.2	15	20	8	8	5	10	6	6	15	20	
13	1.3	15	20	9	9	5	10	6	6	15	20	
3rd Ball is used as a reference as 2nd Ball is lost												
14	1.4	15	20	4	4	5	10					
15	1.5	15	20	5	5	5	10	4	4			4th Ball appeared
16	1.6	15	20	6	6	5	10	4	4	15	20	
17	1.7	15	20	7	7	5	10	4	4	15	20	
18	1.8	15	20	8	8	5	10	4	4	15	20	
19	1.9	15	20	9	9	5	10	4	4	15	20	
4th Ball is used as a reference as 3rd Ball is lost												
20	2.0	15	20	6	6	5	10					
21	2.1	15	20	7	7	5	10	6	6			5th Ball appeared
22	2.2	15	20	8	8	5	10	6	6	15	20	
23	2.3	15	20	9	9	5	10	6	6	15	20	
5th Ball is used as a reference as 4th Ball is lost												
24	2.4	15	20	4	4	5	10					
25	2.5	15	20	5	5	5	10	4	4			6th Ball appeared
26	2.6	15	20	6	6	5	10	4	4	15	20	
27	2.7	15	20	7	7	5	10	4	4	15	20	
28	2.8	15	20	8	8	5	10	4	4	15	20	
29	2.9	15	20	9	9	5	10	4	4	15	20	
6th Ball is used as a reference as 5th Ball is lost												
30	3.0	15	20	6	6	5	10					
31	3.1	15	20	7	7	5	10	6	6			7th Ball appeared
32	3.2	15	20	8	8	5	10	6	6	15	20	
33	3.3	15	20	9	9	5	10	6	6	15	20	
7th Ball is used as a reference as the 6th Ball is lost												
.												
.nth Ball is used as reference when (n-1)th Ball is lost												

vehicle, thereby providing improved safety in the event of collisions with exterior objects. Furthermore, the suggested sensor has a clear advantage over traditional sensors in that it is contactless and unaffected by ambient factors like temperature, density, salinity, or chemical characteristics. It is essential to remember that mathematical equations and ideal physics served as the foundation for the computer simulation. Real-world situations could provide different outcomes.

4. Conclusion

In conclusion, we introduced a captivating proposal for a conceptual model of a novel speed sensor capable of directly measuring the horizontal speed of water and air vehicles relative to the ground. The use of computer simulation to validate the model is a crucial step in assessing its feasibility and performance. The key points of our proposal are direct ground speed measurement: The ability to directly measure the ground speed of water and air vehicles is a significant advantage, as ground speed is often more relevant for navigation and operational purposes. In addition, environmental independence is a major improvement over current speed sensors that rely on contact with the operational environment. This independence can potentially lead to more accurate and reliable speed measurements. In a nutshell, our proposal showcases a promising approach to overcome the limitations of current speed sensors in water and air vehicles. It addresses important challenges

related to ground speed measurement and environmental dependence. If successful, this new speed sensor could bring significant advancements to the field of navigation and enhance the safety and efficiency of water and air vehicles.

References

1. Griswold, W. Lyman, "Underwater logs," Navigation: Journal of the Institute of Navigation, vol. 15, no. 2, pp. 127-135, Summer 1968.
2. C. G. Smith, and j. Slepian, "Electromagnetic vessel's log," U.S. Patent 1249530, Dec. 11, 1917.
3. R. J. Paredes, Quintuña, M. T. M. Arias-Hidalgo and R. Datla, "Numerical flow characterization around a type 209 submarine using OpenFOAM" Fluids, vol. 6, no. 2, pp. 1-23, Feb. 2021, Art. No. 66.
4. The American Practical Navigator: Bowditch, Paradise Cay Publications, Bethesda, MD, USA, 2010.
5. P. Gloaguen, M. Woillez, S. Mahévas, Y. Vermard, and E. Rivot, "Is speed through water a better proxy for fishing activities than speed over ground," Aquatic Living Resources, vol. 29, no. 2, pp. 1-8, Oct. 2016, Art. No. 210.
6. J. Mcorlly, "Pilot Tube," U.S. Patent 2399370, Apr. 30, 1946.
7. Mechanics of flight, Pearson Education Limited, Harlow, ESX, UK, 2006.
8. Principles Of Flight: Aircraft General Knowledge, Flight Performance and Planning (Private Pilot's Licence Course), Airplan Flight Equipment Ltd, Wythenshawe, MCR, UK, 2005.
9. Tietjens, O.K.G. & Prandtl, L. 1957 Applied Hydro and Aeromechanics: Based on Lectures of L. Prandtl, vol. 2. Courier Corporation.
10. Fluid Flow Handbook, McGraw-Hill Professional, Blacklick, OH, USA, 2002.
11. W. Gracey, "Measurement of aircraft speed and altitude," NASA Langley Research Center, Hampton, VA, USA, Rep No. NASA-RP-1046, May 1, 1980.
12. A. Pinker and C. Smith, "Vulnerability of the GPS Signal to Jamming," GPS Solutions, vol. 29, no. 2, pp. 1-8, Oct. 2016, Art. No. 210.
13. A. Grant, P. Williams, N. Ward and S. Basker, "GPS jamming and the impact on maritime navigation,". The Journal of Navigation, vol. 62, no. 2, pp. 173-187, Apr. 2009.
14. G. Taraldsen, T. A. Reinen and T. Berg, "The underwater gps problem," presented at the Conf. Oceans 2011 IEEE, Spain, Jun. 6-9, 2011.
15. G. Xu, Y. Zhao, K. Xu, H. Xu and Z. Cheng, "A speed measurement method for underwater vehicle based on pulse speedometer and accelerometer," presented at the 23rd Int Conf. Offshore and Polar Engineering, Anchorage, Alaska, Jun. 30 - Jul. 5, 2013.
16. Hwang, J. K., Uchanski, M. and Song, C. K. (2005). Vehicle speed estimation based on Kalman filtering of accelerometer and wheel speed measurements. Int. J. Automotive Technology 6, 5, 475–481.
17. A. Lawrence, "Gyro and accelerometer errors and their consequences," in Modern Inertial Technology, New York, NY, USA: Springer, 1998, pp. 25-42.
18. S. Drake and J. Mclachlan, "Galileo's discovery of the parabolic trajectory," Scientific American, vol. 232, no. 3, pp. 102-111, Mar. 1975.

Authors Introduction

Jakaria Mahdi Imam

He received his B.Eng. degree from Military Institute of Science and Technology, Bangladesh. He is currently enrolled at the University of Malaya's master's program focused on research. His research interest includes emerging naval technologies, inertial navigation system and inertial sensors.

Dr. Mohammad Aminul Islam

He graduated from the National University of Malaysia (UKM), Malaysia, in 2012 with an M.Sc. (research) and in 2015 with a Ph.D. in Electrical, Electronic, and System Engineering. In the Department of Electrical Engineering at the University of Malaya, he now holds the position of Senior Lecturer. Optical materials, semiconductor materials, and energy transportation are his areas of interest in study..

Dr. Norrima Mokhtar

She graduated with a B.Eng. from the University of Malaya and an M.Eng. and Ph.D. from Oita University in Japan. She is presently an Associate Professor at the University of Malaya's Department of Electrical Engineering. Human-machine interaction and signal processing are her areas of interest in research.

Dr. S. F. W. Muhammad Hatta

She graduated from the University of Sheffield, UK, with an M.Eng. in Electrical Electronics Engineering in 2005, the University of Malaya, UK, with an M.Sc. in Microelectronics in 2009, and LJMU, UK, with a Ph.D. in Microelectronics in 2014. She is presently a Senior Lecturer at the University of Malaya's Department of Electrical Engineering. Her areas of interest in research are PUF-based technology in cyber-security, advanced semiconductor modelling and characterisation, wearable electronics, and semiconductor dependability.

Dr. Heshalini Rajagopal

She graduated from the University of Malaya in Malaysia in 2016 with a Master's degree and in 2021 with a PhD from the Department of Electrical Engineering. In 2013, she obtained a B.E. in Electrical. She is an assistant professor at Mila University in Negeri Sembilan, Malaysia, at the moment. Artificial intelligence, machine learning, and image processing are among her areas of interest in study.